Photoacoustic correlation signal-to-noise ratio enhancement by coherent averaging and optical waveform optimization

Sergey A. Telenkov,[a] Rudolf Alwi, and Andreas Mandelis
Center for Advanced Diffusion-Wave Technologies, Department of Mechanical and Industrial Engineering, University of Toronto, Toronto, Ontario M5S 3G8, Canada

(Received 4 April 2013; accepted 30 September 2013; published online 21 October 2013)

Photoacoustic (PA) imaging of biological tissues using laser diodes instead of conventional Q-switched pulsed systems provides an attractive alternative for biomedical applications. However, the relatively low energy of laser diodes operating in the pulsed regime, results in generation of very weak acoustic waves, and low signal-to-noise ratio (SNR) of the detected signals. This problem can be addressed if optical excitation is modulated using custom waveforms and correlation processing is employed to increase SNR through signal compression. This work investigates the effect of the parameters of the modulation waveform on the resulting correlation signal and offers a practical means for optimizing PA signal detection. The advantage of coherent signal averaging is demonstrated using theoretical analysis and a numerical model of PA generation. It was shown that an additional 5–10 dB of SNR can be gained through waveform engineering by adjusting the parameters and profile of optical modulation waveforms. © *2013 AIP Publishing LLC*. [http://dx.doi.org/10.1063/1.4825034]

I. INTRODUCTION

Biomedical applications of laser photoacoustics (PA) have attracted significant interest as a unique imaging modality with high sensitivity to optical absorption contrast that can be used to visualize anatomical structure, chemical composition, and physiological activity of the targeted tissues.[1,2] The conventional method of PA imaging consists of pulsed (nanosecond-long) excitation of a tissue specimen and detection of acoustic transients using a broadband ultrasonic transducer coupled with an appropriate image reconstruction algorithm. The wide adoption of the pulsed PA technique is justified by the relatively high acoustic pressure amplitude (tens of kPa) and submillimeter axial resolution achieved with broadband acoustic signals.[3] The benefits of the nanosecond PA technique come with relatively bulky and expensive laser instrumentation which may be cumbersome in a clinical setting and requires regular maintenance to keep stable performance. Additional difficulties are associated with the need for an optical parametric oscillator (OPO) or a dye laser for wavelength tuning in chromophore-specific imaging applications. Furthermore, the pulse repetition rate (typically 10 Hz) is rather low for real-time image acquisition. As a result, the research and development community has turned its attention to more compact and reliable optical sources, such as laser diodes. Attempts to use laser diodes as pulsed optical sources for PA imaging of tissue chromophores were reported previously.[4,5] Although SNR can be increased by taking advantage of the high pulse repetition rate of laser diodes (up to 1 MHz), the overall performance of diode-based systems has been below the standard technique with Q-switched lasers. Additionally, the finite acoustic time-of-flight associated with subsurface chromophore depths limits the maximum pulse repetition rate that can be used for unambiguous signal detection. To avoid ambiguity of the received acoustic pulses, more sophisticated data processing algorithms are required.[5] Our approach to PA imaging differs significantly from the standard pulsed methods and time domain analysis of acoustic transients. The frequency domain photoacoustic (FD-PA) method was introduced[6–8] as an alternative imaging modality that employs intensity modulated continuous wave (CW) laser sources to generate a PA response. At the heart of FD-PA is a correlation signal processing algorithm which provides an effective mechanism to increase SNR by compressing a sub-ms or ms-long modulated response into a narrow correlation peak. In many respects this technique resembles operation of a radar system and can be called "PA radar imaging" to emphasize the specifics of signal processing and the resulting information which is related to the signal energy rather than amplitude. Our previous treatment of SNR in photoacoustic measurements[9] compared FD-PA modality in relation to the conventional pulsed technique. It was shown that despite significant gain of SNR due to matched filter compression, resulting SNR remained approximately 10 dB below the time domain counterpart. Additionally, it was observed that potential for SNR improvement consists in better optimization of optical irradiation parameters under limitation of the ANSI laser safety standard.[10] In the present paper, we investigate problem of optimization of FD-PA methods in greater detail and provide description of various methods that can be employed to improve SNR of the PA correlation technique with a CW laser source. Specifically, we analyze the correlation signal amplitude with respect to modulation waveform parameters such as waveform profile, duration, and laser power under restrictions imposed by the ANSI standard. The results presented herein can be used for practical implementation of the FD-PA method in biological imaging applications.

[a]Author to whom correspondence should be addressed. Electronic mail: sa.telenkov@gmail.com. Present address: PHAST Imaging, 1B Richview Road, Toronto, Ontario M9A 4M6, Canada.

II. FREQUENCY-DOMAIN PA CORRELATION IMAGING WITH A CW LASER SOURCE

The present section provides a brief description of the frequency domain PA imaging modality and describes typical instrumentation used for imaging experiments. Use of a periodically modulated optical source for the generation of acoustic pressure waves has been known since the discovery of the PA phenomenon over a century ago. Despite its long history, the method of choice for PA imaging consists of a short laser pulse (1–10 ns) excitation and broadband detection of the generated acoustic transients. The current commercial availability of high-power laser diodes with average output power greater than 10 W, their relatively low cost and rugged packaging makes them an attractive alternative for designing PA imaging instrumentation. However, the generation of diode laser bursts with duration less than 100 ns results in pulse energies of several μJ as opposed to ~10 mJ of Q-switched lasers. Obviously, such difference in optical excitation energy creates serious challenges for signal detection that can be partially alleviated by averaging a large number of pulses. An alternative use of laser diodes for spatially resolved imaging consists in modulating the laser source according to a prescribed temporal function and, at the detection stage, using matched filter or cross-correlation processing to compress the received signal. For example, the application of linearly frequency-swept waveforms (chirps) for laser modulation with duration 1 ms and correlation processing yields nearly 40 dB SNR gain.[9] At the same time, the axial resolution is defined by the chirp bandwidth which can be less than 1 mm for bandwidths greater than 2 MHz. A typical setup for FD-PA imaging and the associated signal processing algorithm is shown in Fig. 1.

In our experimental setup, we use a near-IR laser diode model 8800 (Laser Light Solutions, Somerset, NJ) with the wavelength of 808 nm and maximum average power of 12 W. The 1-ms long modulation chirps are continuously generated by an arbitrary function generator (PXI 5442, National Instruments, Austin, TX). The chirped analog signal in the form

$$r(t) = A_r \cos(2\pi f_1 t + \pi b t^2), \tag{1}$$

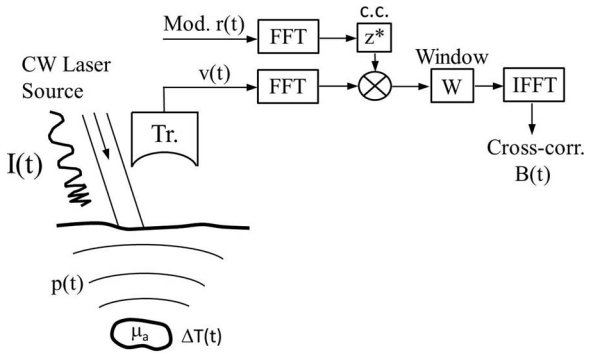

FIG. 1. Schematic of PA imaging with chirped optical excitation and the associated block-diagram of matched filter signal compression (Tr – ultrasonic transducer, FFT – Fast Fourier transform, C.C. – complex conjugate, B(t) – cross-correlation function).

where A_r is a constant amplitude, f_1 is the chirp starting frequency, and b [Hz/s] is the chirp sweep rate, is sent to the laser diode driver. A copy of the modulation waveform is stored in the computer memory and is used as a reference signal in correlation processing. The laser diode output is modulated according to $r(t)$ and is delivered to the tissue surface through an optical fiber. Choice of the chirp frequency sweep range depends on several factors including: transducer spectral sensitivity (transfer function), estimated dimensions of the targeted chromophores, and the chromophore depth. Instead of a single element transducer, an ultrasonic transducer array probe can be used in connection with appropriate multi-channel data acquisition hardware and a beamforming algorithm for image reconstruction.[11] Cross-correlation processing is implemented in the frequency domain using computationally efficient fast Fourier transforms (FFT). Initially, the received transducer signal $v(t)$ and the modulation waveform $r(t)$ are FFT transformed, then the cross-correlation is computed as a product of the signal Fourier spectrum $V(\omega)$ and the complex conjugate of the reference, $R^*(\omega)$. In the final stage, the inverse FFT (IFFT) is computed to yield the time domain cross-correlation function $B(t)$. This processing algorithm can be written in a continuous form as

$$B(t) = \frac{1}{2\pi}\int_{-\infty}^{\infty} W(\omega) R^*(\omega)\, V(\omega)\, e^{i\omega t} d\omega, \tag{2}$$

where $W(\omega)$ is a spectral windowing function applied to the correlation spectrum to reduce range sidelobes. In the ideal case of exact matching, i.e., $V(\omega) = R(\omega)$ and a uniform window, Eq. (2) yields an auto-correlation function, with the peak $B(t = 0)$ being equal to the total energy E_V of the chirp

$$B(t = 0) = \frac{1}{2\pi}\int_{-\infty}^{\infty} |V(\omega)|^2 d\omega = E_V. \tag{3}$$

The correlation processing (2) of a coded PA response provides a simple way of compressing the entire energy of the chirped signal into a correlation peak with the width $\Delta t = 1/\Delta f$, where Δf is the chirp bandwidth. For example, the total optical energy of 1-ms chirps emitted by a 10 W laser source is 10 mJ, which is similar to a single pulse of a Q-switched laser. The laser diode output power is an important characteristic that has direct impact on the acoustic wave amplitude and the detection SNR. In biomedical applications laser irradiation is regulated by the safety standard and is limited by the maximum permissible exposure (MPE) measured in J/cm^2. Therefore, PA generation and detection optimization analysis must include the MPE as a limiting factor. Taking into account the MPE for human skin as a function of exposure duration $T(10^{-7}\ \text{s} \le T \le 10\ \text{s})$, the following empirical expression defines maximum optical energy per unit of area:

$$E_{MPE} = C_A \cdot T^{1/4} \quad [\text{J/cm}^2], \tag{4}$$

where the constant C_A depends on the excitation wavelength; for example, $C_A = 1.81$ for $\lambda = 800$ nm and $C_A = 5.5$ for $\lambda = 1064$ nm. Considering a 10-W laser diode as an optical source with chirp duration $T_{ch} = 1$ ms irradiating a circular

spot 5 mm in diameter, the produced optical exposure is equal to 50 mJ/cm^2, which is much lower than the MPE level (322 mJ/cm^2 at $\lambda = 808$ nm and 978 mJ/cm^2 at 1064 nm). Assuming that optical chirps are emitted continuously, then the MPE level will be reached at time

$$T = N_{ch} \cdot T_{ch}, \tag{5}$$

where N_{ch} is the number of chirps, each of duration T_{ch}. Using Eq. (5) for the maximum exposure time, Eq. (4) for the MPE can be recast in terms of N_{ch} for given laser irradiance I_L [W/cm^2] and T_{ch},

$$C_A(T_{ch}N_{ch})^{1/4} = I_L T_{ch} N_{ch}$$

or

$$N_{ch} = T_{ch}^{-1}\left(\frac{C_A}{I_L}\right)^{4/3}. \tag{6}$$

The above equation defines the maximum number of laser chirps that can be used within the biological laser safety limit. The number of N_{ch} received signals can be averaged to increase the detection SNR. Two possibilities for data averaging are applicable to FD-PA measurements and are considered below.

III. SNR IMPROVEMENT THROUGH COHERENT AVERAGING

Averaging multiple signals is the standard technique for reducing the random noise level and increasing SNR. Since the frequency of acoustic waves is relatively low and ultrasonic transducers are capable of phase-resolved measurements of the PA response, two alternative averaging schemes can be employed: (1) the raw pressure signals can be averaged *coherently* prior to signal processing; or (2) each of the received chirps is processed independently and the resulting correlation amplitudes are averaged. The latter technique does not take into account the phases of individual chirps and constitutes *incoherent* averaging during post-processing. These two methods define the logistics of data acquisition and may influence design of system hardware and software for efficient signal processing. The former technique demands strict phase consistency of multiple excitation chirps and accumulation of multiple waveforms, while the latter allows for rapid processing of incoming chirps and summation of the final products to reduce noise. Both methods of signal conditioning are well known and have been thoroughly analyzed in the theory of radar detection.[12] The difference of the two averaging modes on the resulting correlation SNR can be shown considering an ideal matched filter with the frequency response $H(\omega) = V^*(\omega)$. Initially, we consider SNR gain due to matched filter processing of a single chirp. Defining SNR as a ratio of instantaneous signal power to noise variance σ_N^2, the SNR at the receiver input can be written as

$$SNR_{IN} = \frac{v^2}{\sigma_N^2}. \tag{7a}$$

Following the processing algorithm (2), the correlation output SNR is given by

$$SNR_{OUT} = \frac{B^2(0)}{\sigma_B^2} = \frac{E_V^2}{\sigma_B^2}, \tag{7b}$$

where $\sigma_B{}^2$ is the variance of the correlation noise. Assuming that input noise can be modeled by a zero-mean Gaussian distribution, the output noise power can be computed using a linear system transfer function $H(\omega)$. It is convenient to use analytic signal with $\omega \geq 0$ that can be formed by shaping spectrum with the window function $W(\omega)$. The result of the matched filter processing is a complex valued cross-correlation function $B(t)$ with the real and imaginary parts equivalent to the in-phase and quadrature components of the processed signal. The resulting correlation noise power P_N contained in both components as a result of the input noise $\sigma_N{}^2$ can be estimated as

$$P_N = \frac{S_N}{2} \cdot \frac{1}{2\pi}\int_0^\infty \left|\tilde{H}(\omega)\right|^2 d\omega = \frac{S_N}{2} \cdot E_V = \frac{\sigma_N^2}{f_s} E_V, \tag{8}$$

where the one-sided noise power spectral density $S_N/2 = \sigma_N{}^2/f_s$, and f_s is the signal sampling rate. In the final signal processing stage, the cross-correlation amplitude is computed as $|B(t)| = \sqrt{Re^2\{B(t)\} + Im^2\{B(t)\}}$. Since the amplitude computation is a nonlinear operation, the correlation noise is no longer Gaussian but is distributed according to the Rayleigh probability density function.[12] Therefore, the correlation noise expectation value and variance are given by

$$E\{|B_N|\} = \sigma_N\sqrt{\frac{\pi E_V}{2f_s}}, \tag{9a}$$

$$\sigma_B^2 = 0.43\frac{\sigma_N^2 E_V}{f_s}. \tag{9b}$$

According to (9a) and (9b), after matched filter processing the receiver input noise is translated into an elevated baseline (9a) and the noise mean power is given by (9b). Using Eq. (7b) and subtracting the noise offset (9a), the correlation SNR of a single chirp can be computed as

$$SNR_B = \frac{\left(E_V - \sigma_N\sqrt{\frac{\pi E_V}{2f_s}}\right)^2}{0.43\sigma_N^2 E_V} \cdot f_s. \tag{10}$$

In the case of coherent averaging of N_{ch} chirps, the signal amplitude remains the same, while the input noise is reduced by $\sqrt{N_{ch}}$. Replacing σ_N in Eq. (10) by $\sigma_N/\sqrt{N_{ch}}$, the resulting correlation SNR can be written as

$$SNR_B^{coh} = \frac{\left(E_V - \sigma_N\sqrt{\frac{\pi E_V}{2f_s N_{ch}}}\right)^2}{0.43\sigma_N^2 E_V} \cdot f_s N_{ch}. \tag{11}$$

In the case of incoherent or post-processing averaging of N_{ch} chirps, the resulting correlation function can be written as

$$B_{av}(t) = B_V(t) + \frac{1}{N_{ch}}\sum_{i=1}^{N_{ch}} \beta_i(t), \tag{12}$$

where $B_V(t)$ is the correlation function of the received chirp and $\beta_i(t)$ is the Rayleigh-distributed amplitude noise. Calculating the mean and variance of the noise term results in the incoherent SNR,

$$SNR_B^{incoh} = \frac{\left(E_V - \sigma_N\sqrt{\frac{\pi E_V}{2f_s}}\right)^2}{0.43\sigma_N^2 E_V} \cdot f_s N_{ch}. \quad (13)$$

The main difference between the SNRs of the two averaging modes becomes clear upon inspection of Eqs. (11) and (13). Although in both cases the noise power is reduced by N_{ch}, coherent averaging further reduces the correlation baseline by $\sqrt{N_{ch}}$, whereas incoherent averaging does not affect the dc noise level which is proportional to σ_N. The advantage of coherent averaging is demonstrated in Fig. 2 using a one-dimensional numerical model of PA generation and the correlation processing algorithm.

In this numerical example, a laterally infinite plane absorbing layer 5 mm thick with optical absorption coefficient $\mu_a = 4\ cm^{-1}$ was located 4.5 cm from the detection position and 100 consecutive chirps with the frequency sweep range 1–5 MHz (1 ms each) were numerically generated and processed. The computed PA signals were mixed with zero-mean Gaussian noise to simulate an input SNR = −40 dB. The incoherently averaged result of matched filter processing of all 100 chirps is shown in Fig. 2(a). The correlation peak appears at the correct delay time of 30 μs but significant dc offset masks a substantial portion of the correlation signal. This result is consistent with the theoretical prediction Eq. (13) and the baseline level cannot be reduced by increasing the number of averaged signals. Alternatively, coherent averaging of the raw data followed by correlation processing of single averaged chirps is shown in Fig. 2(b). In agreement with Eq. (11) the resultant noise power is the same as in Fig. 2(a), but the latter plot has the dc background reduced by $\sqrt{N_{ch}}$. The baseline difference between the two averaging modes is important when the PA signals are weak and SNR is very poor, which is usually the case with a modulated CW laser source. In summary, to maximize the SNR of correlation measurements it is advantageous to fix the phases of the optical chirps and coherently average as many of them as allowed by the laser safety limit before processing the output signals.

IV. OPTIMIZATION OF OPTICAL MODULATION WAVEFORM PARAMETERS

Another way of improving the SNR of PA correlation imaging is through optimization of the laser modulation waveform parameters. There are several parameters related to optical chirps including modulation frequency sweep range, chirp duration, and amplitude related to the laser power. These parameters can be adjusted in order to increase the SNR and improve the overall image quality. With respect to chirp frequency range optimization, any *a priori* available information about tissue optical absorption and scattering coefficient, depth of targeted chromophores and frequency response (transfer function) of the ultrasonic transducer is important. Assuming that the chirp frequency range is determined by an ultrasonic transducer and fixed, further optimization of the correlation SNR with respect to the laser power, chirp duration, and waveform profile can be made. The previously used 1-ms duration was set from empirical considerations and it is not guaranteed to be optimal with respect to the resulting SNR. Equations (3) and (10) suggest that longer chirp duration results in greater signal energy content E_V and should yield a higher correlation peak and better SNR. Similarly, an increase of the optical power will produce higher PA response and SNR. However, it has been mentioned that PA imaging of biological tissues *in-vivo* must consider the laser safety restriction (4) that relates laser irradiance to exposure time. Taking into account Eqs. (4)–(6) we analyze the effect of chirp duration T_{ch} on correlation SNR, assuming that the laser irradiance $I_L(T_L)$, where the laser exposure time $T_L = T_{ch}N_{ch}$ is maintained at the safety limit. The correlation SNR dependence on chirp duration was observed experimentally and was briefly discussed in our previous report.[9] Detailed analysis confirms these observations and provides quantitative estimates on SNR optimization that can be achieved by varying the laser chirp parameters. Theoretically, the SNR dependence on chirp duration T_{ch} can be derived using Eq. (3) for the correlation signal amplitude and Eqs. (7) and (8) for the noise power. Since the amplitude of the reference modulation chirp A_r remains fixed, according to Eq. (8) the noise power after matched filter processing becomes

$$P_N = \frac{1}{2\pi}\frac{S_N}{2}\int_{-\infty}^{\infty} |H(\omega)|^2 d\omega \sim E_R \sim T_{ch}, \quad (14)$$

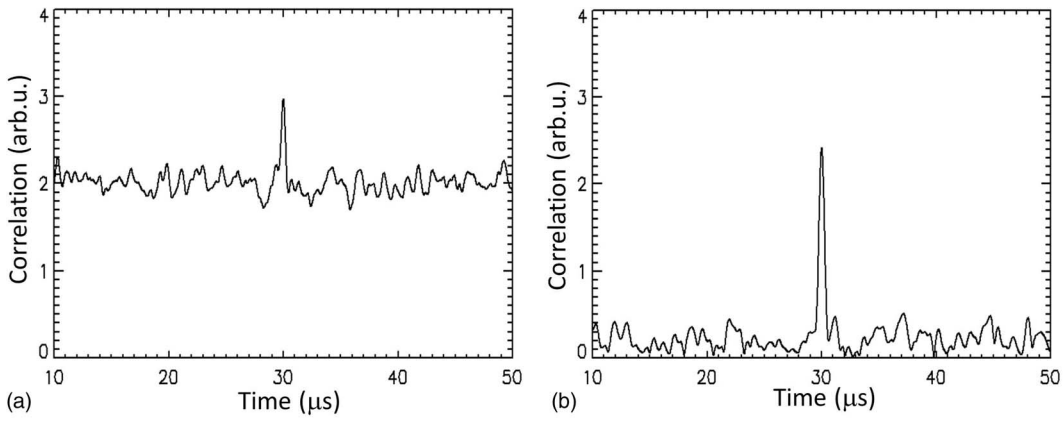

FIG. 2. Numerical analysis of incoherent and coherent averaging of multiple PA chirps showing their effects on the correlation amplitude signal. (a) incoherent and (b) coherent averaging of 100 chirps. Input SNR = −40 dB in both cases.

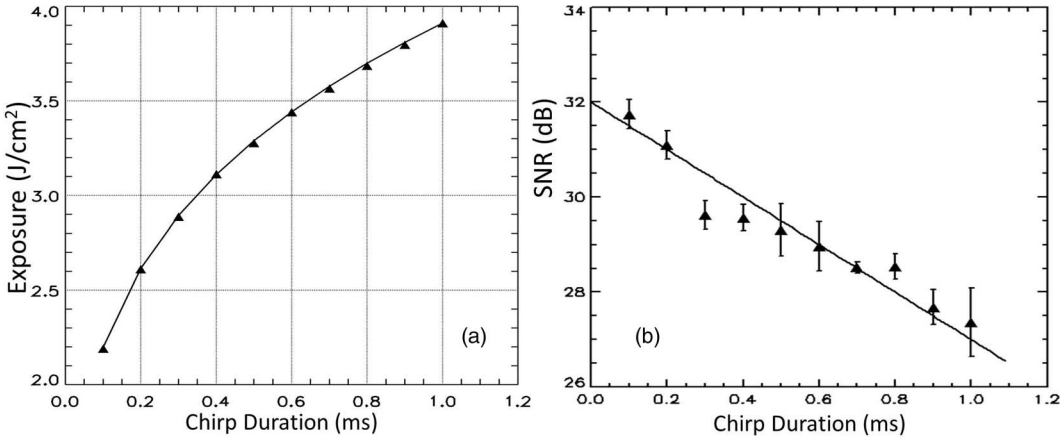

FIG. 3. Measurements of correlation SNR as a function of chirp duration T_{ch}. (a) Laser safety curve (solid) and ▲ – laser exposure used in the measurements; (b) Correlation SNR *vs* chirp duration (solid line $\sim {T_{ch}}^{-1/2}$).

where E_R is the energy of the reference signal. Furthermore, the photoacoustic wave amplitude A_v is proportional to the laser irradiance I_L, which implies that the cross-correlation peak, at time $t = 0$ is

$$B\,(0) \sim A_r A_v T_{ch} \sim I_L T_{ch}. \tag{15}$$

Since the laser irradiance must conform to the MPE limit given by Eqs. (4)–(6), I_L must have the following T_{ch} dependence:

$$I_L = C_A \cdot T_{ch}^{-3/4}. \tag{16}$$

Substituting I_L from Eq. (16) to (15), it is found that the correlation amplitude peak depends on T_{ch} as $B(0) \sim {T_{ch}}^{1/4}$. Taking into account the noise power in Eq. (14), the resulting correlation SNR can be written as

$$SNR_B = \frac{B^2(0)}{P_N} \sim T_{ch}^{-1/2}. \tag{17}$$

This analysis confirms our earlier observation[9] and explains the relation between correlation SNR and the duration of laser chirps. Equation (17) shows that, with respect to correlation SNR, shorter chirp duration is preferred when the laser irradiance varies strictly according to the safety curve $I_L(T_{ch})$ given by Eq. (16). On the other hand, shorter chirps have smaller time-bandwidth product and, as a result, the magnitude of the correlation peak is reduced. Since any decrease of chirp duration must be accompanied by a compensating increase of laser irradiance, the feasibility of this optimization method is limited by the available power of commercial laser diodes.

To verify the theoretical predictions, a series of rigorous measurements was conducted using a planar chromophore ($\mu_a = 2\ \mathrm{cm}^{-1}$) immersed in light-scattering Intralipid solution (reduced scattering coefficient $\mu_s{}' = 10\ \mathrm{cm}^{-1}$) at 15-mm depth.

To generate PA signals, the laser source was modulated by chirped sine waveforms with frequency sweep range f = 1–5 MHz. The experimental setup was similar to that shown in Fig. 1 with a single-element focused transducer (focal distance 2.5 cm, maximum response at 3.5 MHz). The number of signal chirps acquired and averaged was computed from Eq. (6) taking into account the maximum irradiance I_L available from the laser. In this experiment, the number of acquired chirps was set to $N_{ch} = 256$ and was kept fixed. The chirp duration was varied from 100 μs to 1 ms, while the laser irradiance I_L ranged between 12.9 and 72.5 W/cm^2. The total exposure time $T_L = T_{ch}N_{ch}$ was consistent with the MPE limit. The experimental results are shown in Fig. 3. The plot in Fig. 3(a) shows the safety curve (solid line), while triangles indicate the exposure level for each chirp duration. Measurements of the correlation peak and noise power were carried out for each I_L value and the corresponding T_{ch}. Results of the SNR measurements are shown in Fig. 3(b). In agreement with the theoretical analysis predicting SNR $\sim {T_{ch}}^{-1/2}$ (solid line in Fig. 3(b)), it was observed that SNR could be increased approximately by 5 dB when chirp duration was reduced by an order of magnitude. At the same time, the peak magnitude decreased by a factor of 10. This may be detrimental to signal quality and reliable detection, if PA signals are accompanied by strong coherent interference. Typically, coherent interference signals result from direct exposure of the transducer to laser beam and is frequently observed in experiments where the same surface is used for irradiation and detection ("reflection" geometry). In our experiments with the current instrumentation, the range T_{ch} = 500 μs −1 ms was identified as most appropriate for imaging applications.

V. SNR OPTIMIZATION BY THE LASER MODULATION WAVEFORM PROFILE

In addition to adjusting chirp duration and amplitude, the waveform profile can also be changed from sine-wave to a different function of time. The modulation method and specific instruments used in an experiment define the modulated optical output. For example, rapid chopping of the optical beam will produce a nearly square wave profile, while pumping a laser diode with repetitive pulsed current can generate a train of laser pulses with high repetition rate but low duty cycle. In order to quantify the effect of a specific modulation pattern on the correlation amplitude for SNR optimization, we completed a series of measurements with a planar absorber

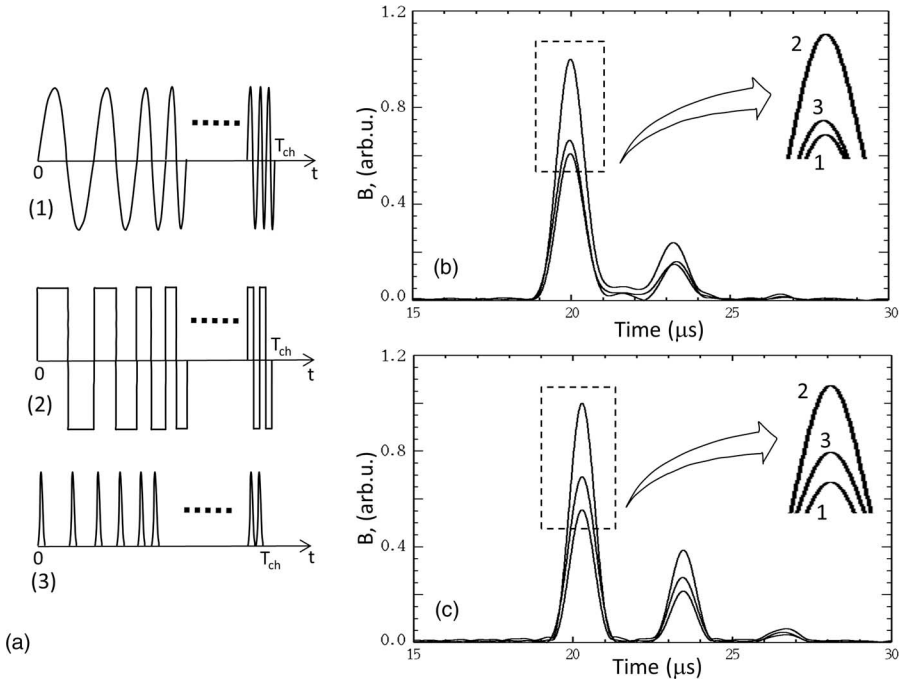

FIG. 4. Effect of modulation waveform profile on the PA correlation signal. (a) Modulation signals: 1 – sine-wave chirp, 2 – square-wave chirp, and 3 – chirped pulse train; (b) Experiment and (c) theory.

and compared the results with a one-dimensional numerical model. Three specific modulation waveforms were investigated: (1) a sine-wave chirp with frequency sweep range 500–2.5 MHz; (2) a square-shaped waveform with 50% duty cycle and the repetition frequency varying linearly in the same range; and (3) a train of pulses with fixed 160-ns duration and there petition frequency varying linearly in the same 500–2.5 MHz range. The optical modulation waveforms and the obtained results of correlation processing are shown in Fig. 4.

In the experiment, a planar absorber (black ink stained polyvinyl chloride (PVC) phantom) with thickness 5 mm and absorption coefficient $\mu_a = 2$ cm^{-1} was placed in clear water at the distance of 3 cm from the transducer. Laser irradiance was set at the 36.8 W/cm^2 and chirp duration at 1 ms for all three modulation waveforms ensuring the same amount of optical energy was incident on the targeted chromophore. To keep laser exposure under the MPE level, 79 signals were recorded and coherently averaged to reduce noise. The processed correlation signals for the three modulation patterns are shown in Fig. 4(b). It was observed that pure sine chirps yield the lowest correlation peak. A small increase (about 10%) in the correlation peak signal occurred when the modulation profile was changed to the pulse train, while the square wave modulation waveform exhibited nearly 65% increase over sine waves. These results were confirmed by a numerical simulation for an absorbing layer with the same optical parameters and dimensions (Fig. 4(c)). Acoustic pressure signals were computed for three irradiation waveforms under the condition that total optical energy remains fixed. The predicted correlation amplitude for the square wave chirp was almost twice as high as for sine wave modulation, in good agreement with the experimental findings. In summary, the highest correlation signal was observed for the square wave modulation waveform. Given that the overall energy of all three waveforms was the same, the observed PA correlation peak magnitude difference can be attributed to differences in the frequency spectra of the modulation signals and the corresponding PA responses. A similar conclusion was arrived at by Farrow *et al.*[13] in their study of single-frequency modulated piezoelectric photoacoustic signals. The chirped results show that approximately 6 dB in correlation signal strength can be gained by changing the modulation profile from pure sine-wave to square-wave, while the chirp sweep range remains the same.

VI. CONCLUSIONS

The commercial availability of high-power laser diodes with a variety of wavelengths in the near-IR spectral range provides an attractive alternative for designing compact PA imaging instrumentation suitable for biomedical applications. Although we have demonstrated that spatially resolved PA imaging with a CW laser source is feasible, the very small amplitude of photo-generated acoustic waves demands particular attention to the detection SNR. The present work demonstrated several practical principles that can be put forward in order to optimize the SNR of PA correlation measurements. It was shown that a standard signal averaging technique can produce different results if coherent build-up of raw PA signals is used as opposed to simple summation of the resulting data. It was also shown that taking into account the laser MPE, the correlation SNR depends on the duration of sine-wave chirps as $1/\sqrt{T_{ch}}$. Therefore, shrinking the chirp duration by an order of magnitude with concomitant increase of the laser irradiance can provide SNR increases of approximately 5 dB. An additional 5–6 dB of correlation SNR can be gained by

changing the modulation temporal waveform from sine-wave to square-wave chirp. More complex modulation signals such as phase-coded waveforms can also be used but their main disadvantage is their relatively short duration and, as a result, the relatively small compression ratio which can seriously limit SNR.

ACKNOWLEDGMENTS

This work was supported by the Natural Sciences and Engineering Council of Canada (NSERC) though Discovery and Strategic grants; by the Premier's Discovery Award, Ministry of Research and Innovation (MRI), Ontario; by the Canada Foundation for innovation (CFI) and the Ontario Research Fund (ORF); and by the Canada Research Chairs (CRC).

[1]C. Li and L. V. Wang, "Photoacoustic tomography and sensing in biomedicine," Phys. Med. Biol. **54**, R59 (2009).
[2]P. Beard, "Beomedical photoacoustic imaging," Interface Focus **1**, 602 (2011).
[3]K. Maslov, H. F. Zhang, S. Hu, and L. V. Wang, "Optical-resolution photoacoustic microscopy for in vivo imaging of single capillaries," Opt. Lett. **33**, 929 (2008).
[4]T. J. Allen and P. C. Beard, "Pulsed near-infrared laser diode excitation system for biomedical photoacoustic imaging," Opt. Lett. **31**, 3462 (2006).
[5]M. P. Mienkina, C. S. Friedrich, N. C. Gerhardt, W. G. Wilkening, M. R. Hofmann, and G. Schmitz, "Experimental evaluation of photoacoustic coded excitation using unipolar Golay codes," IEEE Trans. Ultrason. Ferroelectr. Freq. Control **57**, 1583 (2010).
[6]Y. Fan, A. Mandelis, G. Spirou, and I. A. Vitkin, "Development of a laser photothermoacoustic frequency-swept system for subsurface imaging: Theory and experiment," J. Acoust. Soc. Am. **116**, 3523 (2004).
[7]S. Telenkov and A. Mandelis, "Fourier-domain biophotoacoustic subsurface depth selective amplitude and phase imaging of turbid phantoms and biological tissue," J. Biomed. Opt. **11**, 044006 (2006).
[8]S. Telenkov and A. Mandelis, "Frequency-domain photothermoacoustics: Alternative imaging modality of biological tissues," J. Appl. Phys. **105**, 102029 (2009).
[9]S. Telenkov and A. Mandelis, "Signal-to-noise analysis of biomedical photoacoustic measurements in time and frequency domains," Rev. Sci. Instrum. **81**, 124901 (2010).
[10]American National Standard for safe use of lasers, ANSI Z136.1, 2007.
[11]S. Telenkov, R. Alwi, A. Mandelis, and A. Worthington, "Frequency-domain photoacoustic phased array probe for biomedical imaging applications," Opt. Lett. **36**, 4560 (2011).
[12]J. Minkoff, *Signals, Noise and Active Sensors: Radars, Sonars, Laser Radars* (Wiley-Interscience, New York, 1992).
[13]M. M. Farrow, R. K. Burnham, M. Auzanneau, S. L. Olsen, N. Purdie, and E. M. Eyring, "Piezoelectric detection of photoacoustic signals," Appl. Opt. **17**, 1093 (1978).